

Fractal growth of the liquid crystalline B2 phase of a bent-core mesogen

This article has been downloaded from IOPscience. Please scroll down to see the full text article.

2001 J. Phys.: Condens. Matter 13 1353

(<http://iopscience.iop.org/0953-8984/13/7/302>)

View [the table of contents for this issue](#), or go to the [journal homepage](#) for more

Download details:

IP Address: 171.66.16.226

The article was downloaded on 16/05/2010 at 08:36

Please note that [terms and conditions apply](#).

Fractal growth of the liquid crystalline B2 phase of a bent-core mesogen

Ingo Dierking¹

Department of Physics, Division of Microelectronics and Nanoscience,
Chalmers University of Technology, S-41296 Göteborg, Sweden

E-mail: dierking@hrz2.hrz.tu-darmstadt.de

Received 28 November 2000, in final form 21 December 2000

Abstract

Fractal growth patterns can be observed during the formation of the liquid crystalline B2 phase of a bent-core molecule from the isotropic melt. The time development of the box dimension D_b , the information dimension D_i and the mass dimension D_m was determined during the phase ordering process, as the cell gap, quench depth and quench rate was varied. The fractal dimensions obtained for various growth patterns were of the order of $D \approx 1.82$ – 1.89 in a two-dimensional medium, values which are generally found for percolation clusters in condensed matter systems. The fractal dimension increases for increasing cell gap, but is basically independent on quench depth and rate.

1. Introduction

Since the introduction of fractal geometry by Mandelbrot [1] in the early 1980s, this concept has been successfully employed in the description of various processes of pattern formation in most areas of science, ranging from physics, chemistry and biology to material science, engineering and geology [2]. This includes growth processes of various condensed matter systems, aggregation and percolation systems, viscous fingering and dielectric breakdown patterns, as well as electro-deposition or surfaces and interfaces. Fractal geometry is especially useful in the description of disordered systems, percolation and branched growth patterns [3]. Thus it is surprising, that there are only very few investigations reported for liquid crystalline and related systems. One such report is related to an estimation of the fractal dimension of a dendritic-type texture of a discotic columnar hexagonal ordered phase [4], which bears a certain similarity to patterns formed in viscous fingering, i.e. the Saffman–Taylor instability studied in Hele–Shaw cells of liquid crystals [5–8], although in the latter case the observed structures are not related to a phase ordering process. Other investigations describe a fractally homogeneous distribution of nuclei [9] and topological defects [10, 11] in nematic liquid crystals.

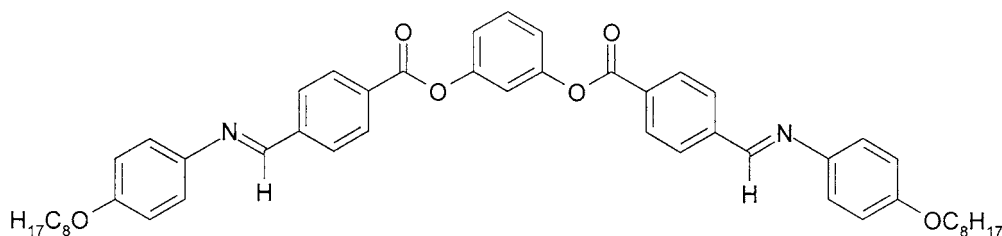
¹ Present address: Institut für Physikalische Chemie, Technische Universität Darmstadt, Petersenstrasse 20, D-64287 Darmstadt, Germany.

Growth structures with a fractal dimension may be obtained by different mechanisms. Two models account for a large number of systems observed in condensed matter, percolation and diffusion-limited aggregation [12]. In percolation systems, clusters are formed by sites being occupied with a certain probability, growth depending on local interactions. Percolation clusters in two-dimensional space are found to exhibit a fractal dimension of the order of $D = 1.89$ at the percolation threshold. In the case of diffusion-limited aggregation, small beads or clusters are initially formed, which diffuse randomly, before they interact to form aggregates of larger size (cluster–cluster aggregation). These are generally more highly branched and exhibit a fractal dimension of the order of $D = 1.7$ in two-dimensional space, often found for aggregation processes of colloidal systems.

In this study, the fractal dimensionality of growth structures, formed during the phase ordering process of a liquid crystal phase after a temperature quench from the isotropic melt, is investigated for a bent-core or so called ‘banana’-molecule. The observed patterns are qualitatively different from those of ‘conventional’ calamitic mesogens, which generally exhibit spherical or bâtonnet growth of nematic or smectic nuclei, respectively.

2. Experiment

The compound under investigation was first reported in [13] and has a structural formula as given below:



Phase transition temperatures (in °C) were determined by polarizing microscopy on very slow cooling: Iso. 169.6 B2 150.3 BX 145.5 Cryst. The compound shows a two-phase region of about 3 K at the isotropic to liquid crystal transition, which is quite common for banana-mesogens and may be attributed to impurities. The clearing point T_C (Iso.–B2) was taken as that temperature where first liquid crystalline nuclei were observed on slow cooling.

Growth patterns were studied by use of polarizing microscopy (Nikon OPTIPHOT2-POL), equipped with a Mettler FP52 hot stage for temperature control better than 0.1 K. Digital images were recorded with imaging software from Bergström Instruments AB and a microscope mounted digital video camera (Sony Hyper HAD model SSC-DC38P) at an image size of 768×576 pixels. For maximum contrast between the isotropic and the B2 phase the camera was driven in slight intensity overload. This procedure assured conversion of digital images without loss of the structural features.

For the investigations, the compound was introduced into commercially available liquid crystal sandwich cells (EHC, Japan) by capillary action in the isotropic phase. General experimental conditions were as follows: image size $1080 \mu\text{m} \times 820 \mu\text{m}$ (corresponding to 768×576 pixels), cell gap $d = 3 \mu\text{m}$, quench depth $\Delta T = 0.3 \text{ K}$ and quench rate $R = 3 \text{ K min}^{-1}$. For the different investigation series only the respective parameter was varied, leaving other conditions unchanged.

Fractal image analysis was carried out with BENOIT 1.3 (Trusoft-International) using several methods.

- (1) *The box dimension method.* This defines the fractal dimension D_b from the exponent in the proportionality

$$N(d) \sim \frac{1}{d^{D_b}} \quad (1)$$

with $N(d)$ the number of boxes of size d being occupied by the data set.

- (2) *The information dimension method.* The fractal dimension D_i is given from the proportionality

$$I(d) \sim -D_i \log(d) \quad (2)$$

with $I(d)$ the information entropy of $N(d)$ boxes of size d , given by

$$I(d) = - \sum_{i=1}^{N(d)} m_i \log(m_i) \quad (3)$$

with $m_i = M_i/M$, where M_i is the number of points in the i th box and M the number of total points in the data set. In contrast to the box dimension method, the information dimension method weights the boxes according to the number of points contained.

- (3) *The mass dimension method,* which yields the fractal dimension D_m , following the proportionality

$$m(r) \sim r^{D_m} \quad (4)$$

with $m(r) = M(r)/M$ the ‘mass’ within a circle of radius r , where $M(r)$ is the data set of points contained within a circle and M the total number of points in the set.

The fractal dimension was in each case determined by minimization of the standard deviation of a linear fit to a log–log plot according to equations (1), (2) and (4) to $SD < 0.001$. For each procedure, the box/radius size was varied over more than two orders of magnitude, resulting in a variation of the dependent variable over more than four orders of magnitude. The linear regime from which the fractal dimensions were determined covered at least one decade in box/radius size.

3. Experimental results and discussion

Figure 1 depicts a typical growth evolution of the liquid crystal B2 phase (bright) from the isotropic liquid (black), with images taken every 10 s apart. Images were recorded at isothermal conditions after a temperature quench to $\Delta T = 0.3$ K below the clearing point for a cell of gap $d = 3 \mu\text{m}$. During the phase ordering process, only a few clusters are formed, which grow and eventually coalesce into larger aggregates. Analysing the images of figure 1, the fractal dimension of individual clusters was found to be constant within the limits of error and equal to the dimension determined for the whole microscopic texture, as shown in figure 2. Coalescence of isolated clusters did not change their fractal dimension. These observations, together with a value of $D \approx 1.83$, suggests that the growth of the liquid crystalline B2 phase from the isotropic melt is accomplished by percolation clusters, rather than diffusion-limited aggregation.

For the following investigations, the whole microscopic field of view ($1080 \mu\text{m} \times 820 \mu\text{m}$, corresponding to 768×576 pixels resolution) was used for fractal dimensional estimation. A set of illustrative data of the fractal analysis of figure 1(f) is shown in figure 3 for (a) the box dimension method, (b) the information dimension method and (c) the mass dimension method. All methods yield comparable results: $D_b = 1.85$, $D_i = 1.83$ and $D_m = 1.86$. In all cases, the fractal dimension was determined for a variation of the box/radius size dimension by more

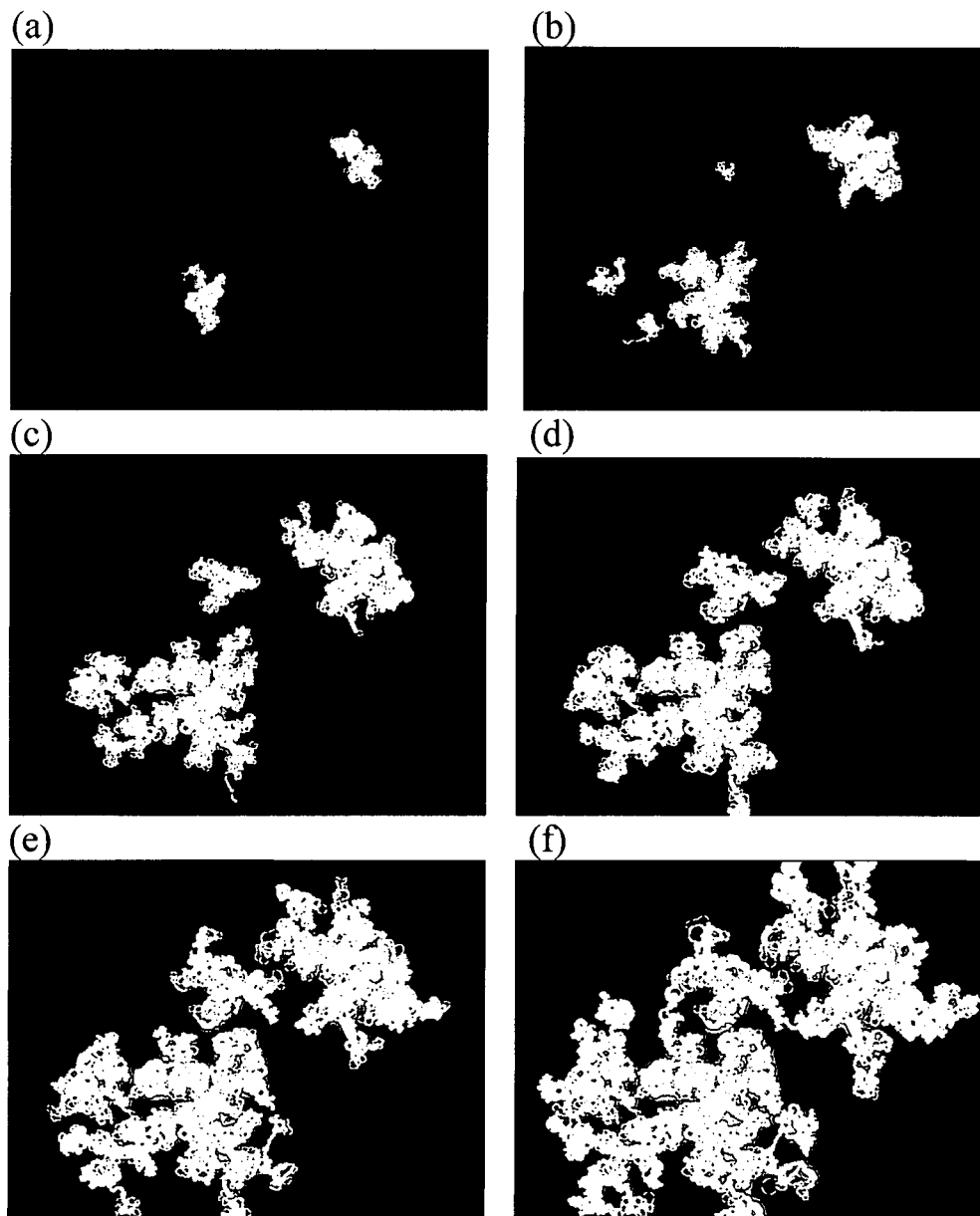


Figure 1. Exemplary series of fractal growth patterns at isothermal conditions at quench depth $\Delta T = 0.3$ K in a $d = 3$ μm cell. The image size is 1080 $\mu\text{m} \times 820$ μm each, taken at time intervals of 10 s.

than one order of magnitude, corresponding to at least two orders of magnitude on the scale of occupied boxes/points within the circle.

Figure 4(a) shows the time development of the fractal box dimension D_b for several cell gaps. A clear increase of D_b with time can be observed for all cell gaps in the interval of 2 $\mu\text{m} < d < 15$ μm until a saturation dimension $D < 2$ is reached. The saturation value of the fractal dimension, obtained by all three different methods employed, increases for increasing

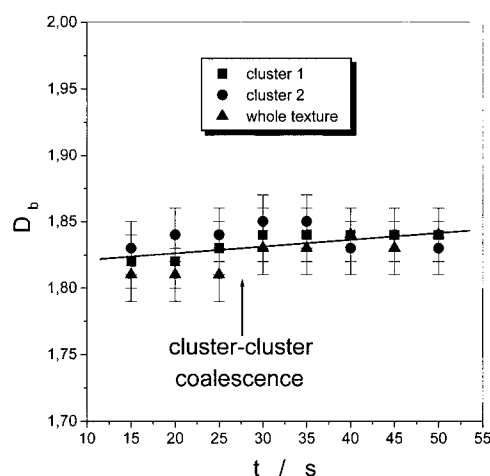


Figure 2. Fractal dimension of different B2 clusters (squares, circles) as a function of time of isothermal phase ordering, including coalescence of individual clusters (squares, $t > 30$ s), in comparison with an analysis of the whole texture (up triangles), observed during growth of the liquid crystalline B2 phase from the isotropic melt. Fractal analysis is referring to the image series depicted in figure 1.

cell gap below $d = 8 \mu\text{m}$ (figure 4(b)). Above a cell gap of approximately $8 \mu\text{m}$, a constant fractal dimension is observed, possibly indicating a vanishing influence of the substrates on the liquid crystal phase ordering process.

Figure 5(a) illustrates the time development of the fractal box dimension for different quench depths ΔT below the Iso.-B2 transition at constant cell gap $d = 3 \mu\text{m}$ and quench rate $R = 3 \text{ K min}^{-1}$. Also here, a strong increase of D_b with values of the order of $D = 1.6$ for short times can be observed with time, until saturation is reached after approximately 1 min at isothermal conditions with $D \approx 1.87$. Possibly, this behaviour might illustrate a change from growth below the percolation threshold at short times, for which $D = 1.56$ is obtained theoretically, to one at the percolation threshold at longer times, for which $d = 1.89$ is predicted. For increasing quench depth the saturation value of the fractal dimension is obtained at shorter times. This is accounted for by the well known fact that the phase ordering process proceeds more quickly at larger super-cooling. A more detailed account of the saturation fractal dimension as a function of quench depth is given in figure 5(b) for all three methods employed. Within the limits of error, the fractal dimension remains constant at a value of approximately $D \approx 1.87$, as the quench depth ΔT is increased. This implies that the observed growth structures are basically independent on growth velocity.

In a third series, the fractal dimension of the B2 growth structures was investigated as a function of quench rate R at constant cell gap $d = 3 \mu\text{m}$ and quench depth $\Delta T = 0.3 \text{ K}$. Intuitively, one would expect that the quench rate does not have any influence on the phase ordering process, as long as this proceeds at isothermal conditions. The time development of D_b is depicted in figure 6(a). At large quench rates $R > 3 \text{ K min}^{-1}$ and short times $t < 15 \text{ s}$, smaller fractal dimensions are obtained as compared to moderate quench rates. This might be attributed to an insufficient electronic temperature regulation for large cooling rates, not imposing isothermal conditions at all times of the phase ordering process. In any case, the saturation value of the fractal dimension, as determined by all three methods employed, is independent of quench rate (figure 6(b)), as expected, and of the order of $D \approx 1.88$.

For all investigation series, phase ordering of the B2 phase of the bent-core mesogen was

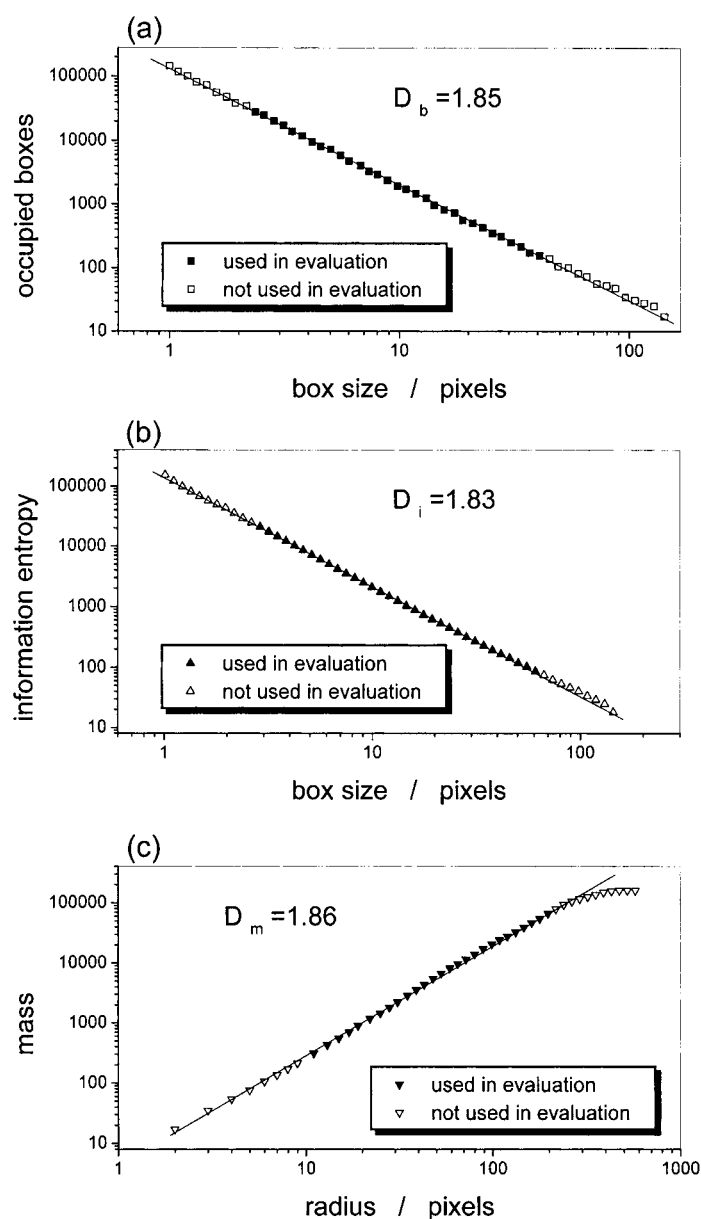


Figure 3. Exemplary illustration of the determination of the fractal dimension by minimization of the standard deviation of data obtained for the image of figure 1(f): (a) box dimension method, (b) information dimension method and (c) mass dimension method.

accomplished by the formation of only a few nuclei, which grow in a complex fashion, leading to clusters with an average fractal dimension of the order of $D \approx 1.87$. Under no conditions the transition was accomplished by coalescence of numerous small 'islands', forming complex aggregates. In general, the observed behaviour suggests a growth process via percolation clusters rather than diffusion-limited aggregation, although also a growth process via clustering aggregation, which may lead to similar fractal dimensions, cannot be completely ruled out.

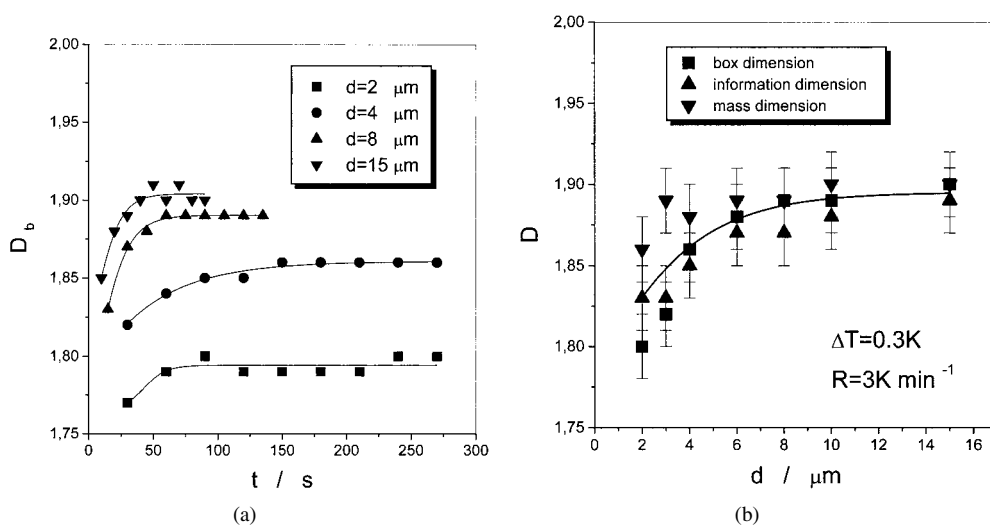


Figure 4. (a) Time development of the fractal box dimension D_b for several different cell gaps d . (b) Dependence of the saturation fractal dimension D on cell gap, determined by different methods (\square : box dimension D_b , \blacktriangle : information dimension D_i , \blacktriangledown : mass dimension D_m).

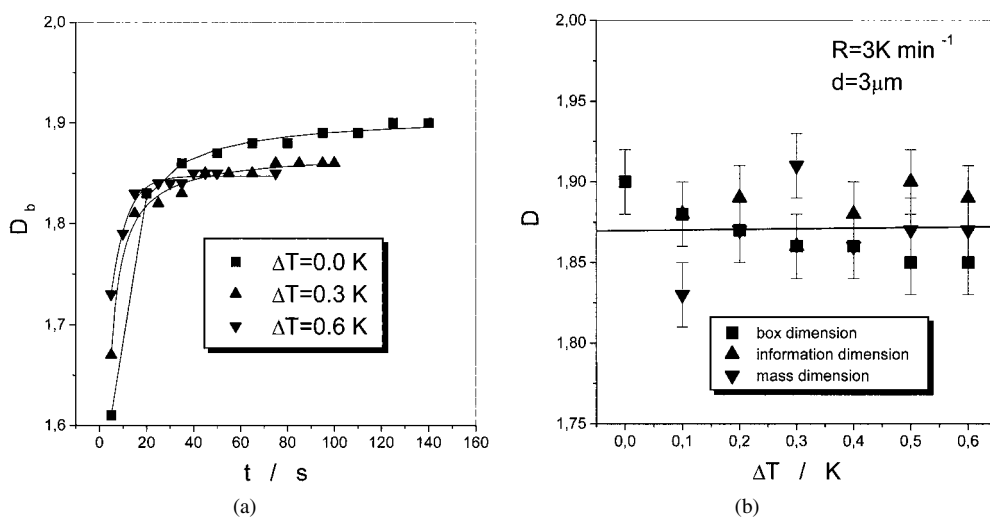


Figure 5. (a) Time development of the fractal box dimension D_b for several quench depths ΔT . (b) Dependence of the saturation fractal dimension D on quench depth, determined by different methods (\square : box dimension D_b , \blacktriangle : information dimension D_i , \blacktriangledown : mass dimension D_m).

4. Conclusions

The evolution of growth structures during the phase ordering process of the liquid crystalline B2 phase of a bent-core molecule from the isotropic melt was studied by determination of the fractal dimension by different methods. The observed growth structures are qualitatively different from those of conventional calamitic mesogens and characteristic for the so called 'banana'-phases. It was demonstrated that different liquid crystalline clusters have the same fractal dimension, which is not changed by coalescence of clusters either. Fractal growth is

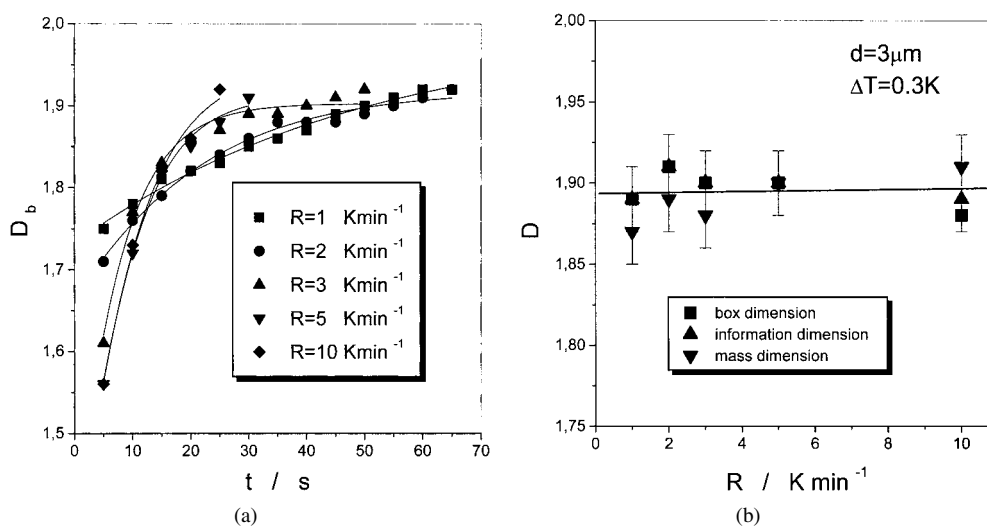


Figure 6. (a) Time development of the fractal box dimension D_b for several quench rates R . (b) Dependence of the saturation fractal dimension D on quench rate, determined by different methods (\square : box dimension D_b , \blacktriangle : information dimension D_i , \blacktriangledown : mass dimension D_m).

influenced by the dimension of the sample, exhibiting an increasing fractal dimension as the cell gap is increased below $d = 8 \mu\text{m}$, while quench depth and quench rate have practically no influence on the dimension of the aggregates observed. Microscopic observation of the growth structures and their average fractal dimension of the order of $D \approx 1.87$ suggest a growth process via percolation clusters.

Acknowledgments

The compound used in this investigation was kindly provided by G Pelzl, Halle. I would also like to acknowledge the financial support of the Fonds der Chemischen Industrie, the Swedish Foundation for Strategic Research and the European Network LCPHOTONET.

References

- [1] Mandelbrot B 1982 *The Fractal Geometry of Nature* (San Francisco: Freeman)
- [2] Bunde A and Havlin S (eds) 1994 *Fractals in Science* (Berlin: Springer)
- [3] Bunde A and Havlin S (eds) 1996 *Fractals and Disordered Systems* 2nd edn (Berlin: Springer)
- [4] Baehr C, Ebert M, Frick G and Wendorff J H 1990 *Liq. Cryst.* **7** 601
- [5] Buka A, Kertesz J and Vicsek T 1986 *Nature* **323** 424
- [6] Horvath V K, Kertesz J and Vicsek T 1987 *Europhys. Lett.* **4** 1133
- [7] Buka A, Palffy-Muhoray P and Racz Z 1987 *Phys. Rev. A* **36** 3984
- [8] Vicsek T 1987 *Phys. Scr. T* **19** 334
- [9] Nakagawa M, Kobayashi K, Hori M, Okabe M and Hori Y 1991 *Mol. Cryst. Liq. Cryst.* **195** 15
- [10] Massalska-Arodz M 1994 *Nukleonika* **39** 77
- [11] Massalska-Arodz M 1998 *Acta Phys. Pol. A* **94** 41
- [12] Daoud M and Van Damme H 1999 *Soft Matter Physics* ed M Daoud and C E Williams (Berlin: Springer)
- [13] Sekine T, Niori T, Sone M, Watanabe J, Choi S W, Takanishi Y and Takezoe H 1997 *Japan. J. Appl. Phys.* **36** 6455